



An Evaluation of Ground Penetrating Radar for Mapping Fracture Networks in the Hawkesbury Sandstone

Never Stand Still

Connected Waters Initiative Research Centre

Richard Rosendorff



*Connected Waters Initiative Research Centre,
School of Biological, Earth and Environmental Sciences
University of New South Wales, Australia*

Contents

- Introduction
 - Current Conflicts
 - The Southern Coalfields
- Objectives
- Survey Areas
- Field methodologies
 - Field Mapping
 - GPR
 - Basics
 - Results
 - Interpretation
- Discussion and Conclusion
- Future Research
- References

Introduction

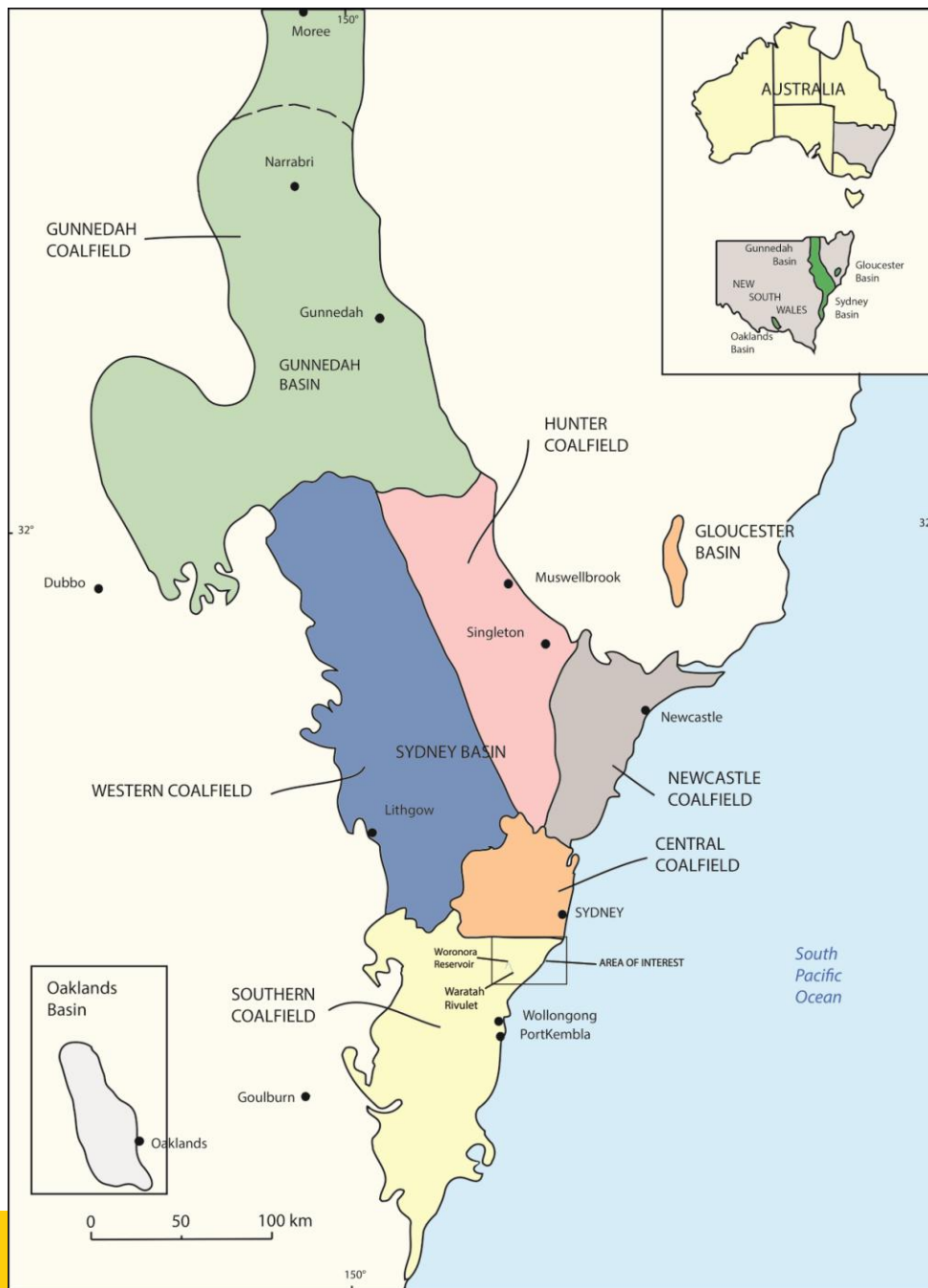
- Subsidence due to longwall coal mining causes fracturing of the overlying rocks.
- When a longwall panel is extracted beneath or adjacent to a stream/river there can be detrimental impacts on the near surface hydrology.
- Longwall mining caused significant fracturing of the bedrock in the Waratah Rivulet. This changed the near surface flow paths, and altered the water chemistry.
- To better assess the impacts we need a good understanding of the changes to the near surface fracture network.
- It has been demonstrated that GPR can map fractures (Heikkinen and Kantia, 2011; Leucci et al., 2007).
- We opted to test the Mala Rough Terrain GPR system.

Current conflicts

- Coal is extensively mined across New South Wales
- Main extraction method is Longwall mining
- Vertical subsidence and Horizontal movements
 - Reduced water quality
 - Growth of iron oxidising bacterial mats
 - Loss of ecological habitats
 - Accelerated bank erosion
 - Extensive gullying erosion
- There are a number of environmental concerns due to continuing longwall mining activities in the Southern Coalfield

The Southern Coalfield

- Located in the Sydney Basin
- Made up primarily of Permian and Triassic sedimentary and volcanic rocks
- Intruded by dykes
- Extensive natural fracture network.
- The only Coalfield in NSW that produces hard coking coal
- Extracted from the Bulli seam at up to depths of 400 m
- Main units above the Bulli seam
 - Hawkesbury Sandstone
 - Narrabeen Group



Waratah Rivulet: Fracturing



Diverted Flow

Waratah Rivulet: Filling of Fractures



Waratah Rivulet: Increased Iron



Objectives

- To evaluate if the Mala Rough Terrain GPR system can be used to map the major and minor joint networks and bedding planes.
- Measure the alteration of fracture networks caused by longwall mining
- Test the capabilities of GPR to detect such features at an unaltered nearby site
- Frequencies tested 100 and 25 MHz

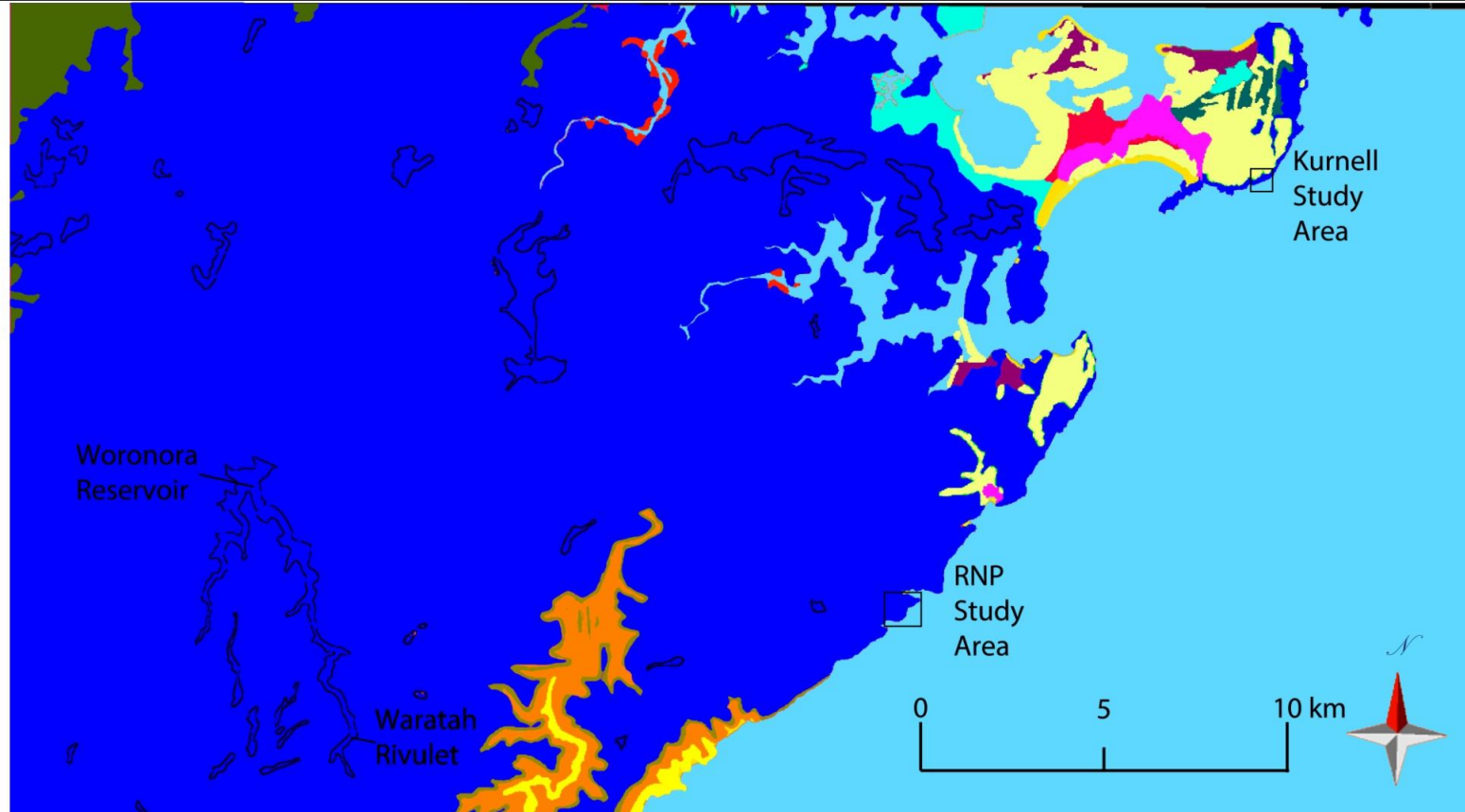
Survey areas

- Areas with extensive visible surface fracturing where chosen
- Parts of
 - The Kurnell Peninsula
 - The Royal National Park
 - Wattamolla
 - Curracurrong
- Fractures were identified from aerial photographs.
- Fractures delineated from the aerial photographs were confirmed in the field.

Geological map of Study area

LITHOLOGY

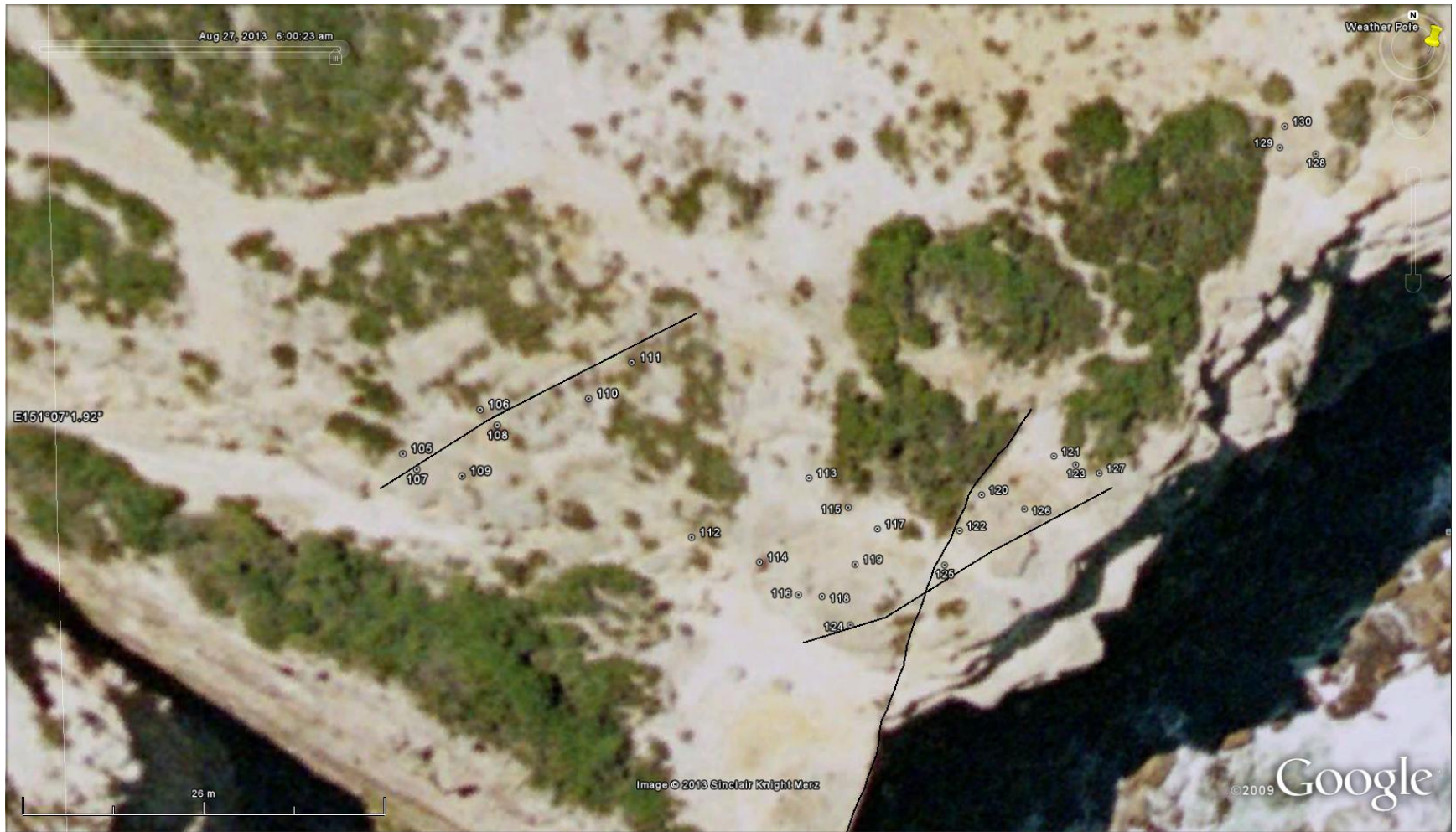
- mf - Man-made fill. Dredged estuarine sand and mud, coal washing, industrial and household waste.
- Qal - Quartz and lithic "fluvial" sand, silt, and clay.
- Qmd - "Marine" quartz sand.
- Qhs - Peat, sandy peat, and mud
- Qhd/Qht - Medium to fine-grained "marine sand with podzols and shelly layers./ Organic-rich muddy, mostly "marine" sand.
- Qtd - Clean to muddy, shelly, mostly "marine" sand, sometimes with low dunes.
- Qbd - Medium to fine "marine" quartz sand with podzols
- Qhb - "Marine" quartz sand, fine to medium shelly. Leached to varying degrees.
- WIANAMATTA GROUP**
- Rwa - Laminite and dark-grey siltstone.
- HAWKESBURY SANDSTONE**
- Rh - Medium to coarse-grained quartz sandstone, very minor shale and laminite lenses
- NARRABEEN GROUP**
- Gosford Subgroup**
- Rnz - Undifferentiated interbedded quartzose and quartz - lithic sandstone and siltstone, clay pellet sandstone.
- Clifton Subgroup**
- Rnbu - Fine to medium-grained quartz-lithic sandstone with lenticular shale interbeds.
- Rnsp - Red, green, and grey shale and quartz-lithic sandstone.



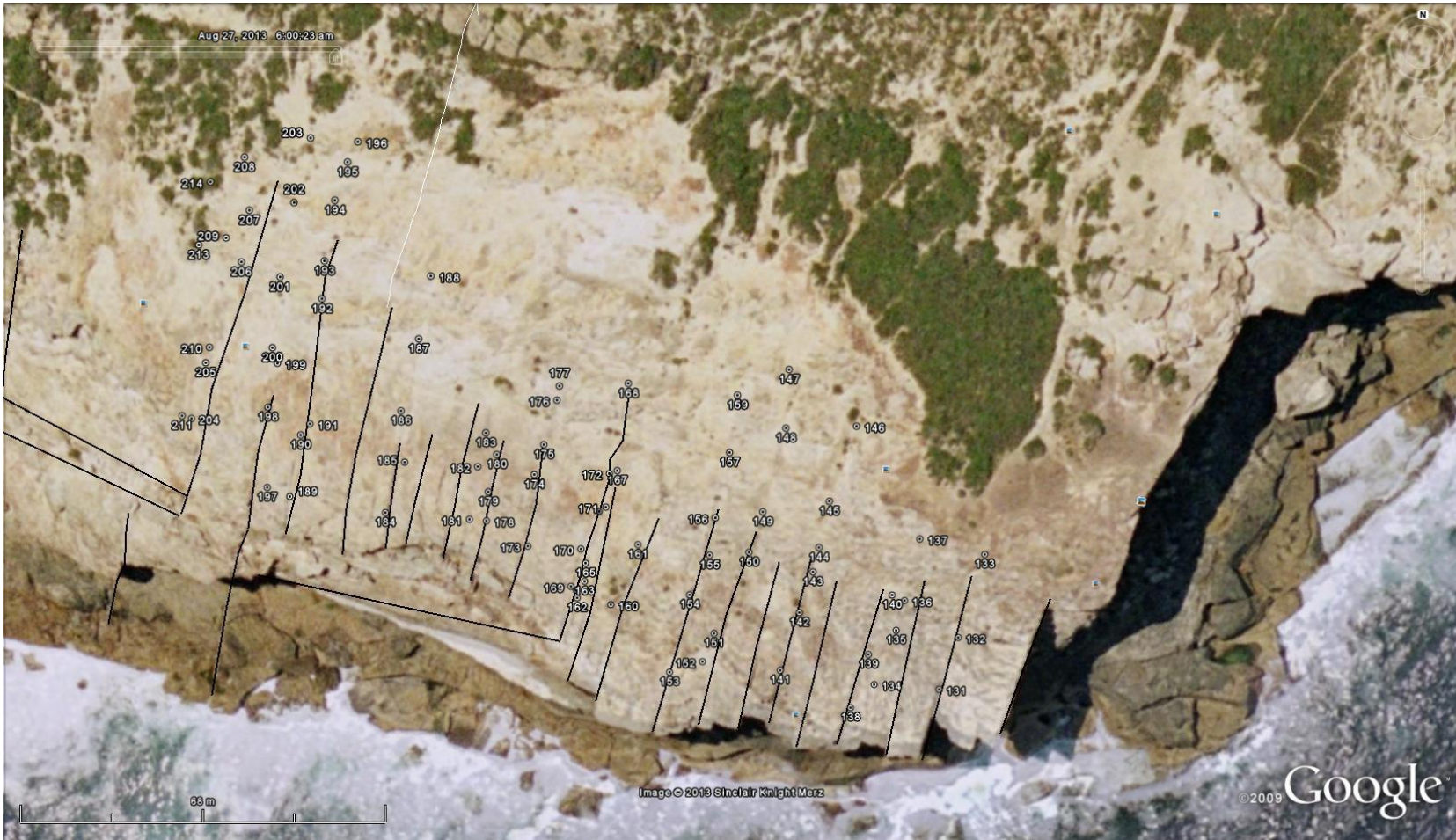
Kurnell survey site



Royal National park North Survey site



Royal National park South Survey site



Fracture mapping

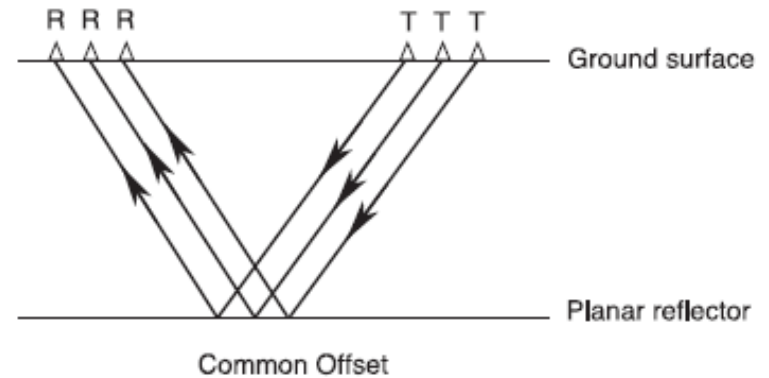
- Average orientation of approximately 190° and 202° at Kurnell and Royal National Park (RNP) sites respectively from aerial photographs
- NNW-SSE orthogonal fracture pattern, in sync with previous findings by Memarian Fergusson (2003) and Shepherd and Huntington (1981)
- Average spacing of fractures mapped (metres)
 - Kurnell – 6.58
 - RNP North – 2.715
 - RNP South – 7.6815
- Field mapping gave ranges of strikes
 - Kurnell – 95° - 226°
 - RNP North – 230° - 245°
 - RNP South – 193° - 202°

Ground-Penetrating Radar (GPR) Basics

- Geophysical technique that allows high resolution imagery of the sub surface (<50m)
- Detects electrical discontinuities in the shallow subsurface
- Emits a pulse of electromagnetic energy and records the time required for the return of any reflected signal
- Reflections are produced from surfaces where there is a sharp contrast in the dielectric constant of the earth materials.
- While some energy is reflected back to the antenna , remaining energy will continue travelling through the material until it attenuates.
- Signal attenuation is dependent on the properties of the material the pulse passes through and the frequency of the GPR antenna

GPR System

- MALA Rough-Terrain Antenna (RTA)
 - 100 Mhz antenna – 2m spacing
 - 25 Mhz antenna – 6 m spacing
- Towed by a single surveyor
- Common offset survey
- Quick and Easy to use























Royal National Park (RNP) Survey Site

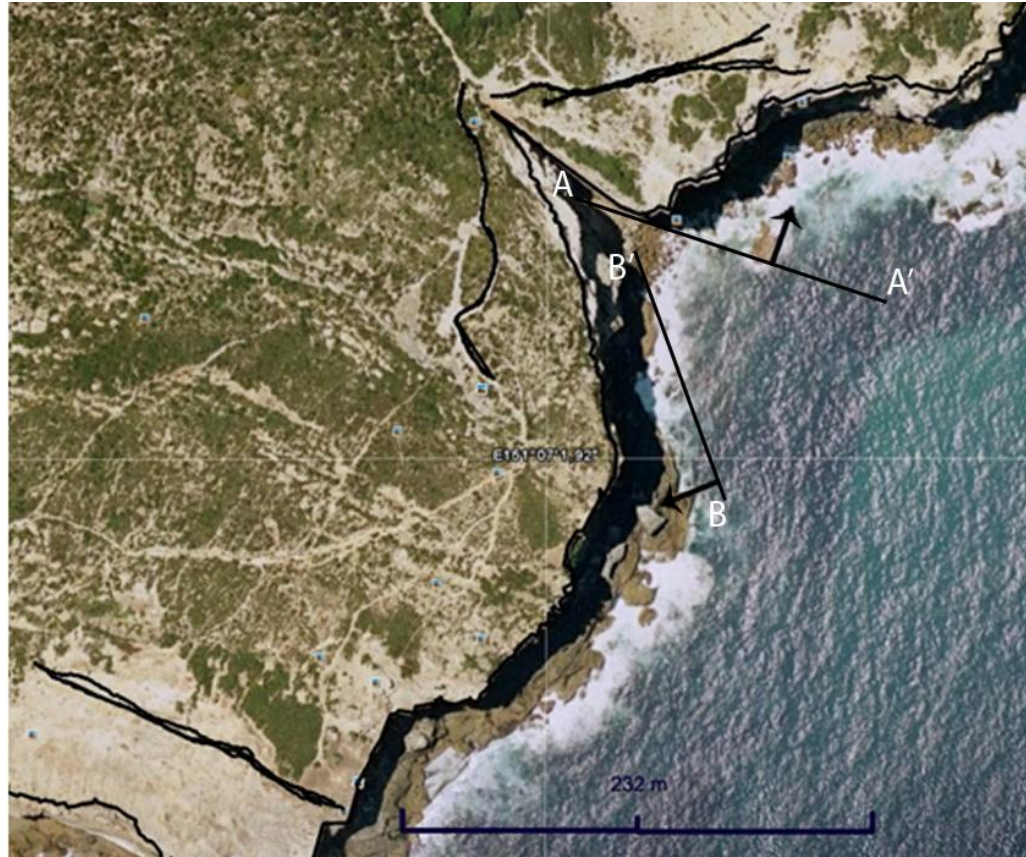


Photo A-A'



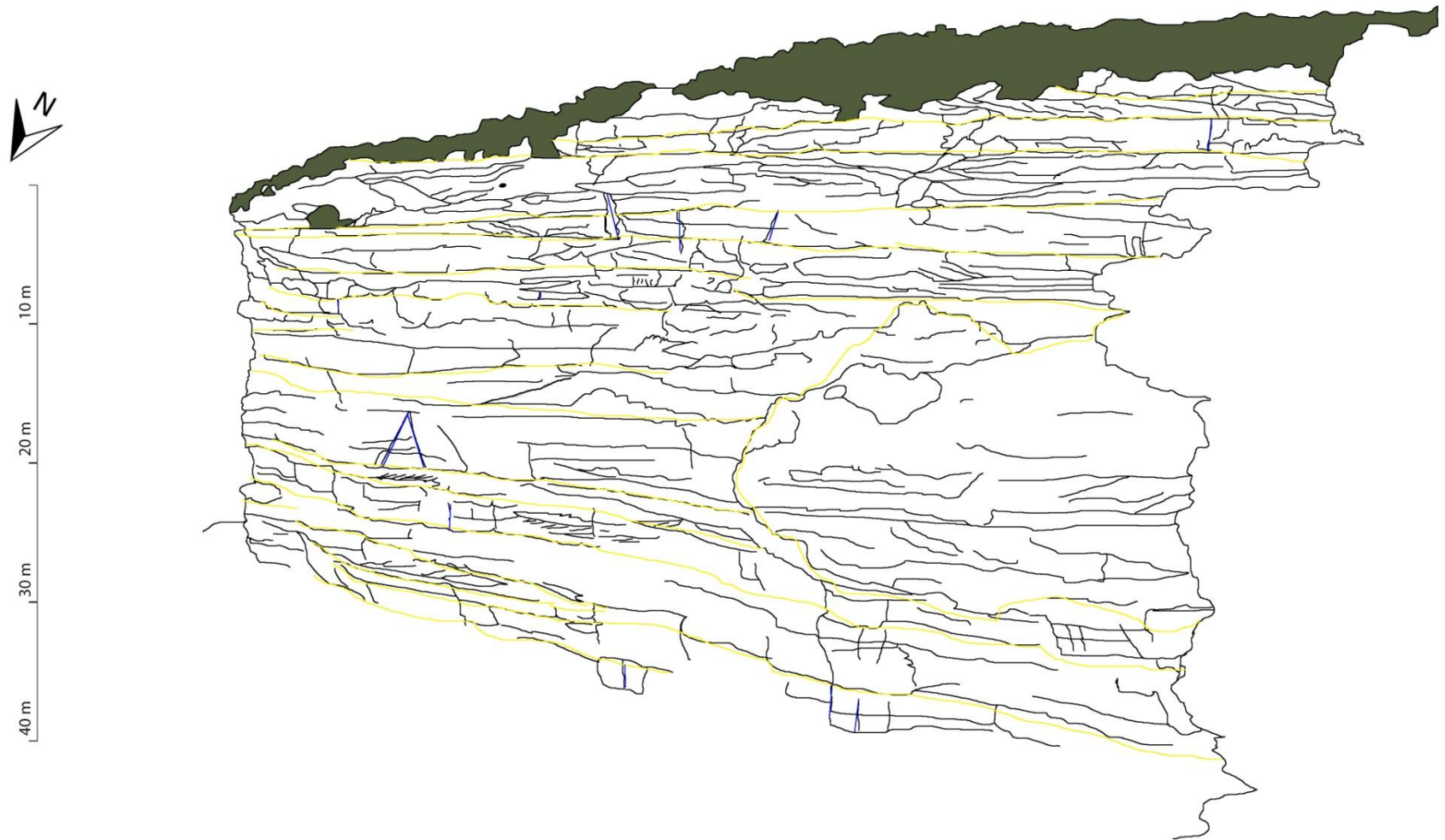
Digitised A-A'



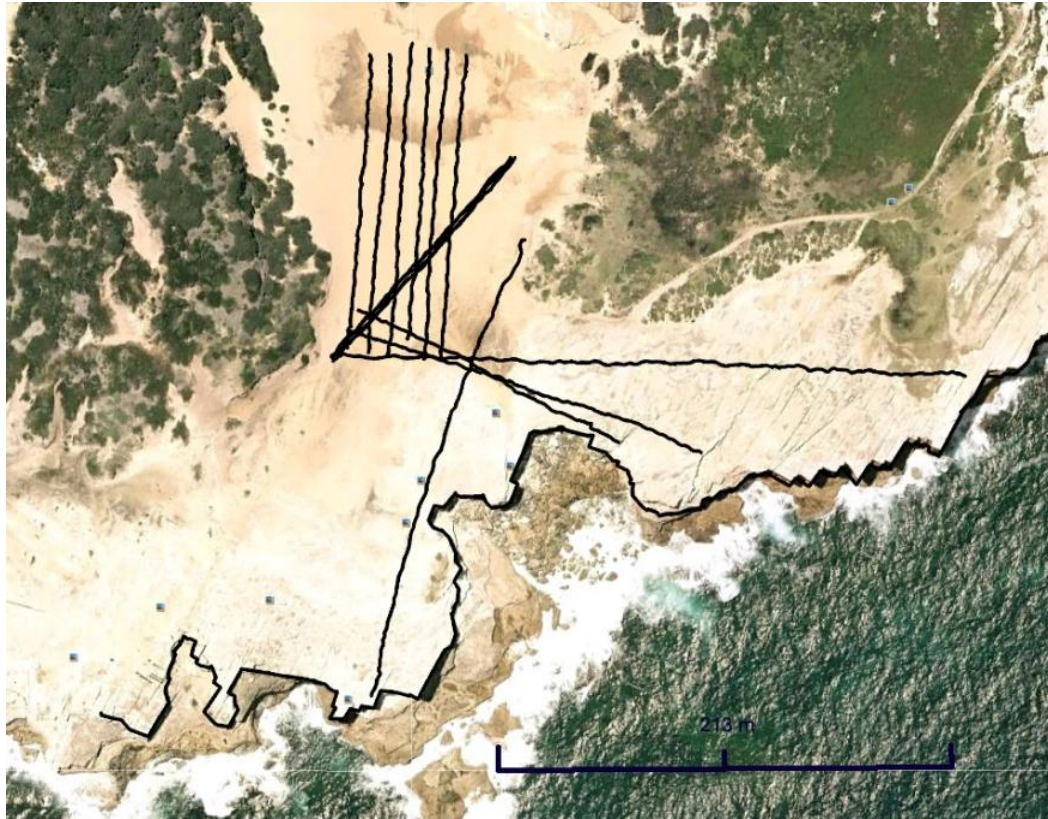
Photo B-B'



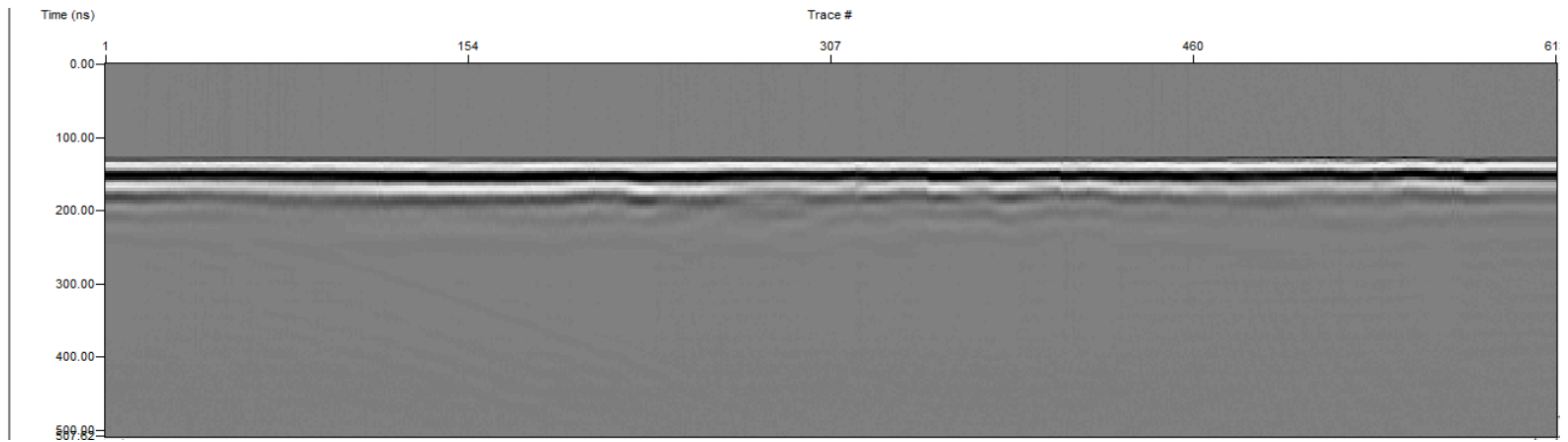
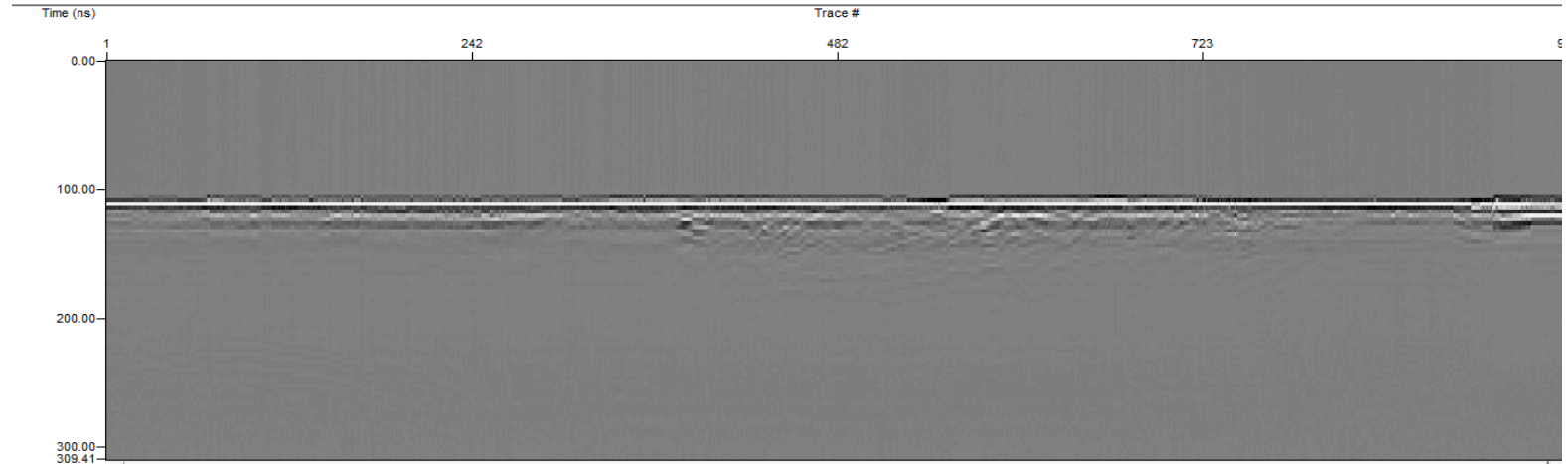
Digitised B-B'



Kurnell Survey Site



GPR Profiles 100 and 25 Mhz RNP North



GPR signal paths

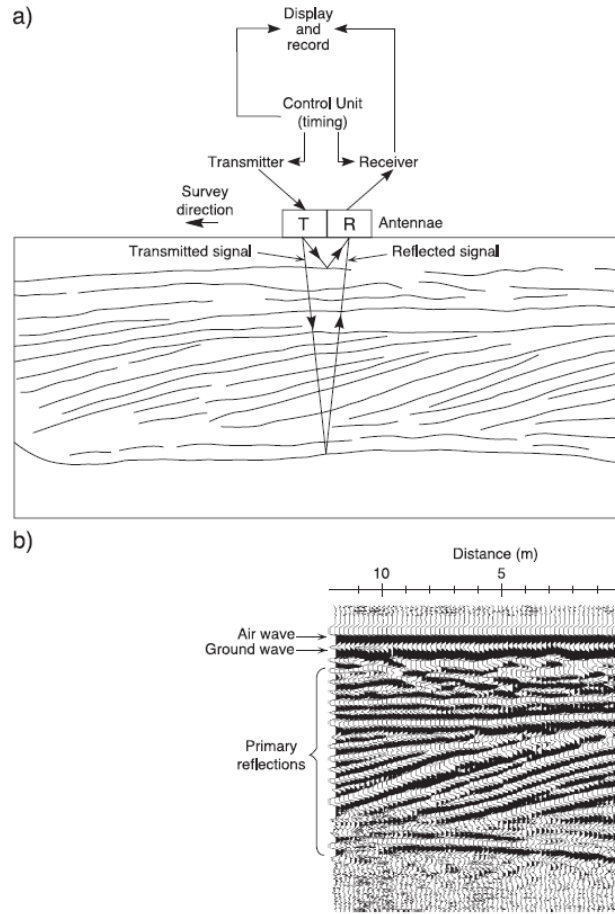


Fig. 3. GPR data acquisition and the resulting radar reflection profile. (a) Data acquisition at an individual survey point, showing GPR system components and subsurface reflector configuration. (b) Radar reflection profile resulting from sequential plotting of individual traces from adjacent survey points. Position of the airwave, ground wave and primary reflections are indicated. Modified from Neal and Roberts (2000).

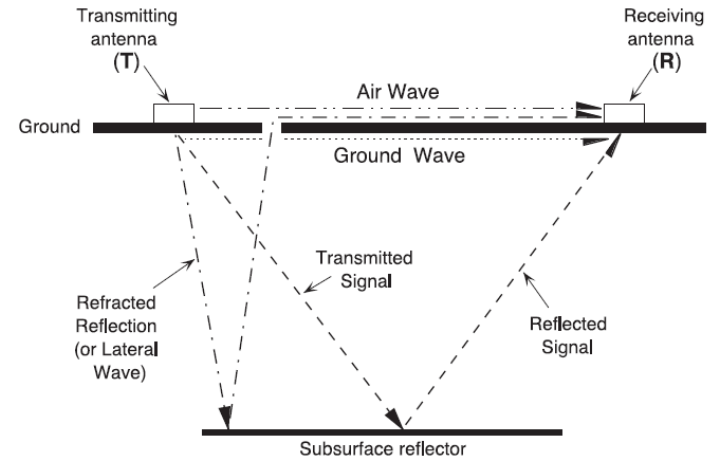


Fig. 4. Ray paths between transmitting and receiving antennae for the airwave, the ground wave, a lateral wave and a reflected wave. Modified from Fisher et al. (1996).

From Neal (2004)

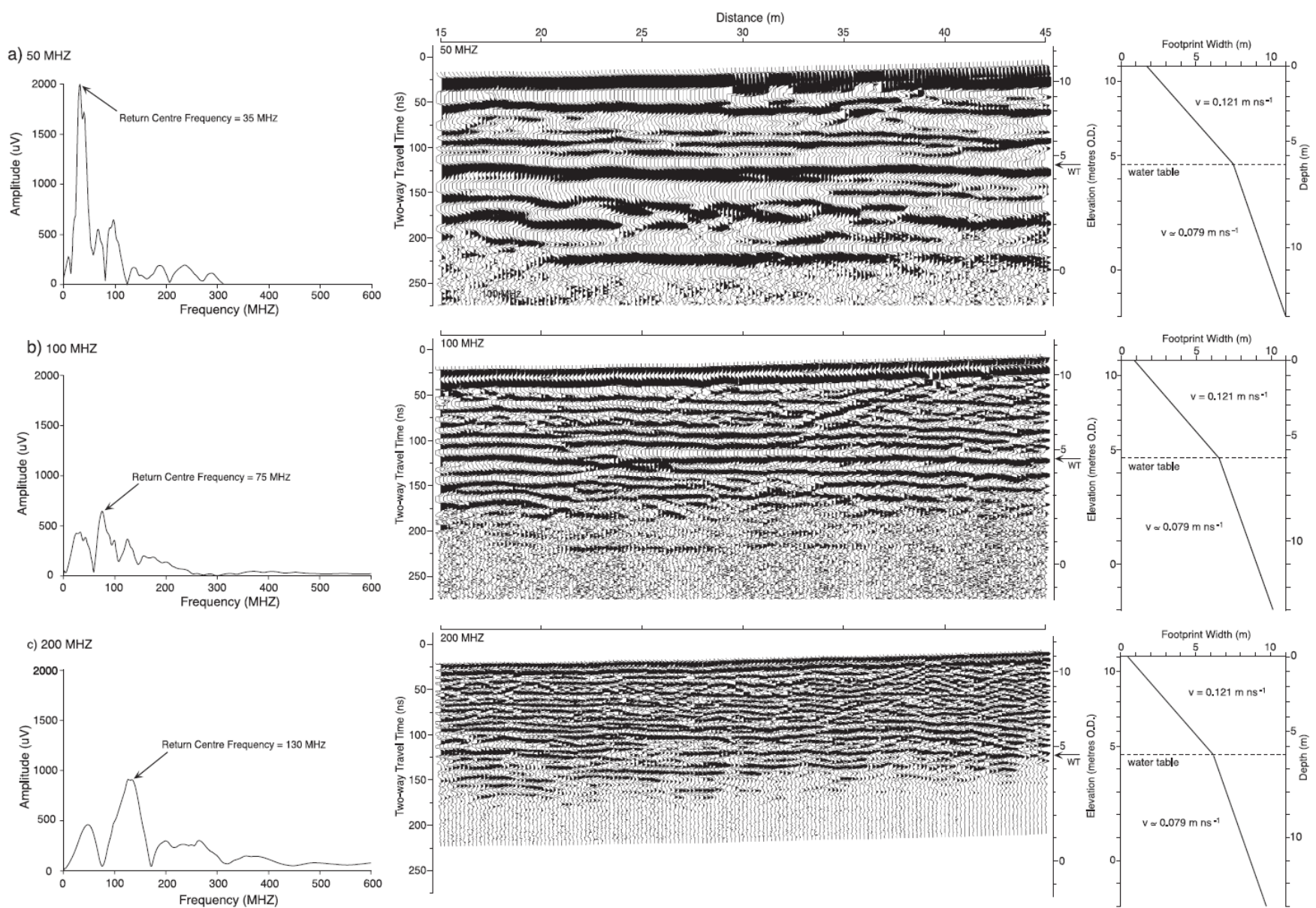


Fig. 7. Return-frequency spectrums, radar reflection profiles and radar-footprint size variations with depth for data collected along the same shore-parallel transect across sand-and-gravel-rich beach ridge-plain deposits, Beckfoot, outer Solway Firth, northwest England using antennae with nominal centre frequencies of (a) 50 MHz, (b) 100 MHz and (c) 200 MHz. Note expansion of the elevation axis beneath the water table (WT) due to the decrease in radar wave velocity.

**Typical Dielectric Constant, Electrical
Conductivity, Velocity and
Attenuation Observed in Common
Geologic Materials**

MATERIAL	K	σ (mS/M)	v (m/ns)	α (dB/m)
Air	1	0	0.30	0
Distilled Water	80	0.01	0.033	2×10^{-3}
Fresh Water	80	0.5	0.033	0.1
Sea Water	80	3×10^3	.01	10^3
Dry Sand	3-5	0.01	0.15	0.01
Saturated Sand	20-30	0.1-1.0	0.06	0.03-0.3
Limestone	4-8	0.5-2	0.12	0.4-1
Shales	5-15	1-100	0.09	1-100
Silts	5-30	1-100	0.07	1-100
Clays	5-40	2-1000	0.06	1-300
Granite	4-6	0.01-1	0.13	0.01-1
Dry Salt	5-6	0.01-1	0.13	0.01-1
Ice	3-4	0.01	0.16	0.01

Annan, P
GPR course notes

POWER REFLECTED

The amount of energy (power) reflected at a dielectric boundary depends on the dielectric contrast. It is calculated from:

$$R = \left(\frac{\sqrt{K_1} - \sqrt{K_2}}{\sqrt{K_1} + \sqrt{K_2}} \right)^2$$

where:

R = power reflected

K_1 = dielectric constant of the first layer

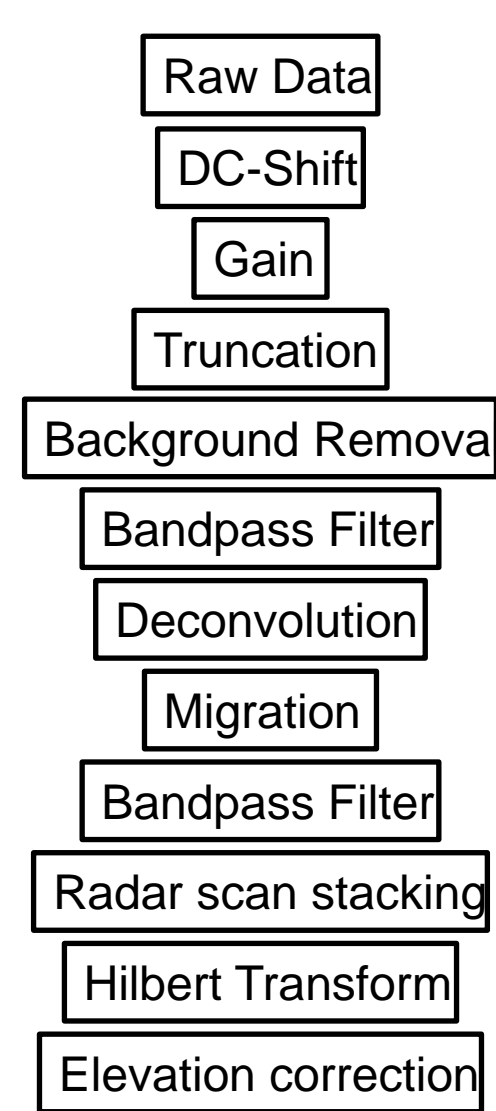
K_2 = dielectric constant of the second layer

Table 1. Power reflected from dielectric boundaries

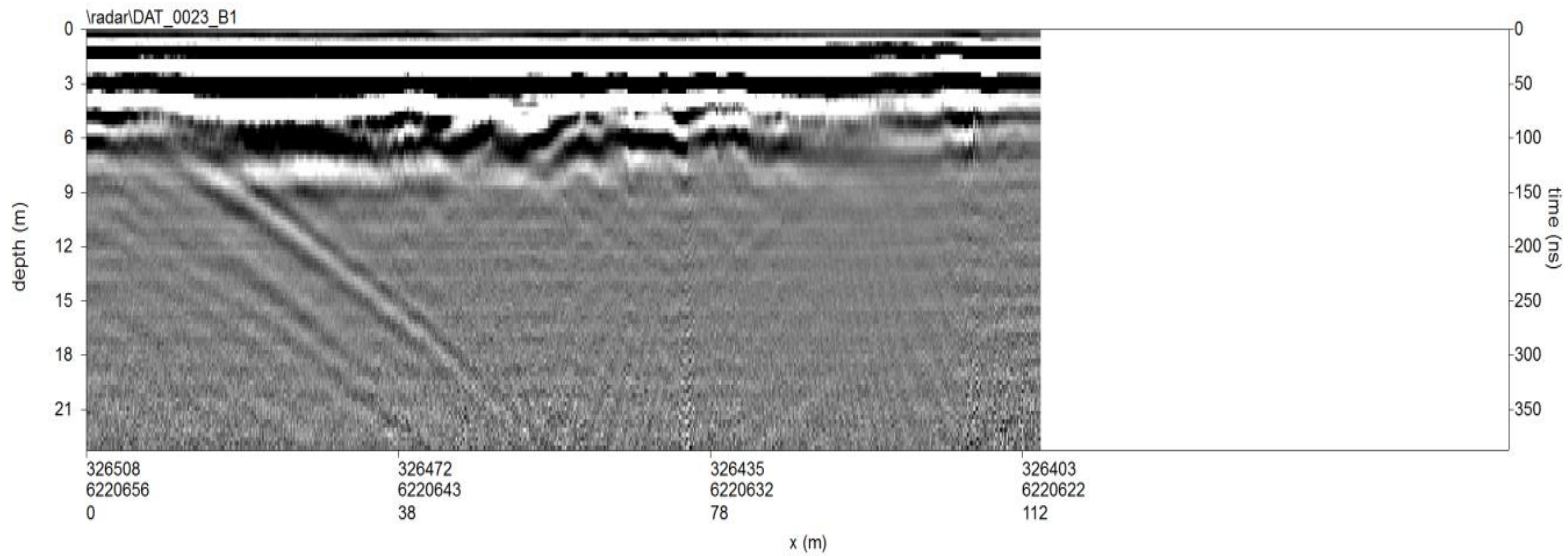
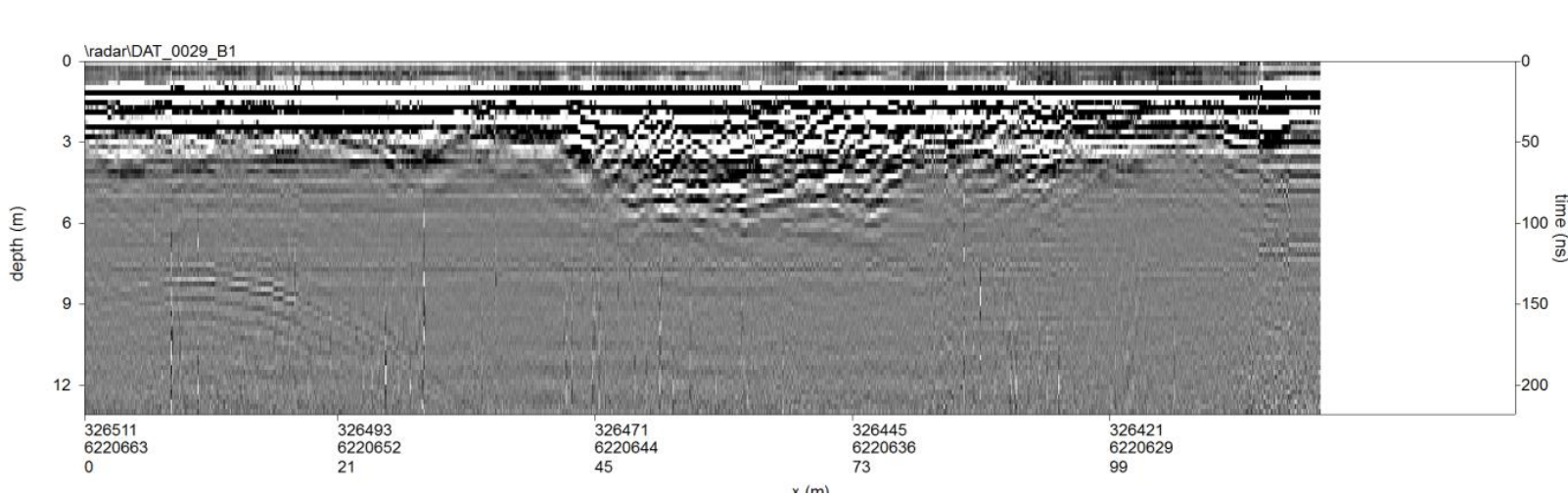
K_1	K_2	R
1	1	0
1	2	0.03
1	5	0.15
1	10	0.27
1	25	0.44
1	50	0.57

GPR data Processing

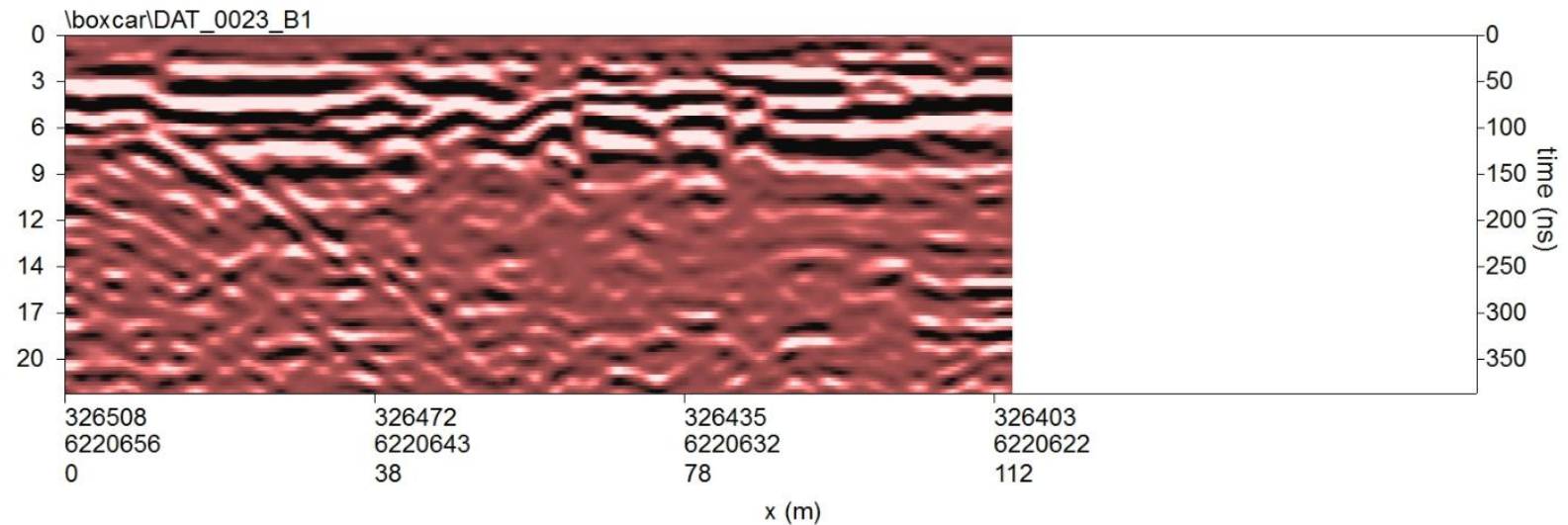
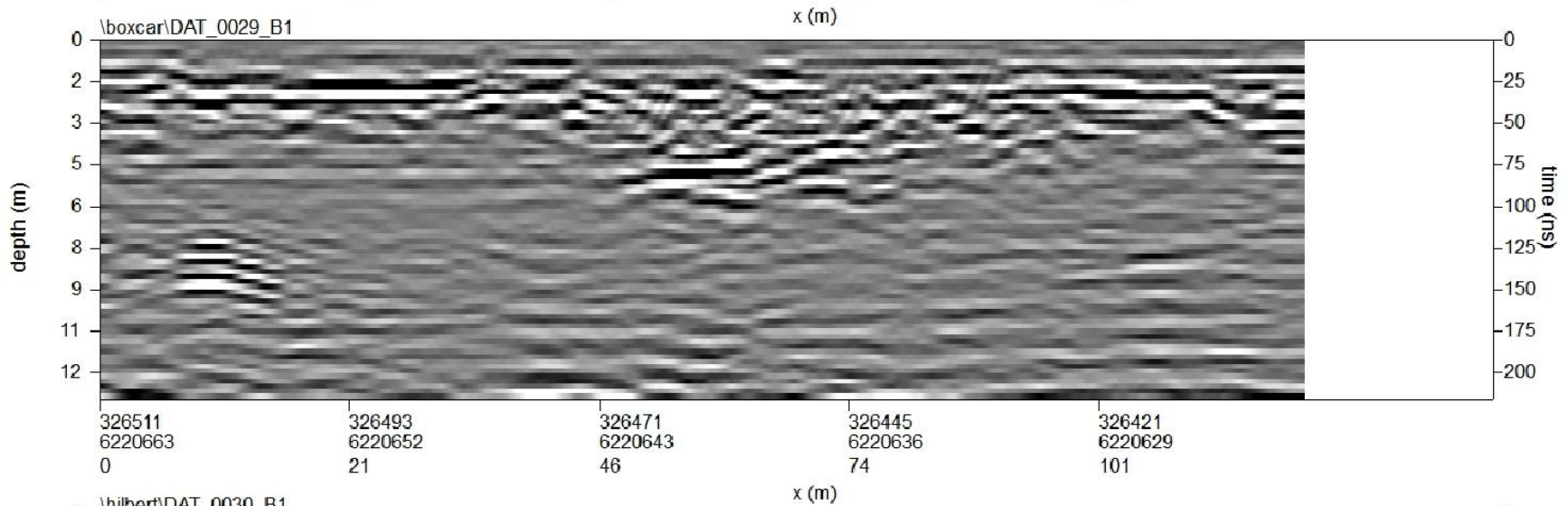
- Processing is applied to
 - Remove horizontal banding
 - filter out noise and enhance reflection events
 - Remove hyperbolae and return reflection events to their original dip
 - Restore the radargram to the correct spatial location



Basic Processing

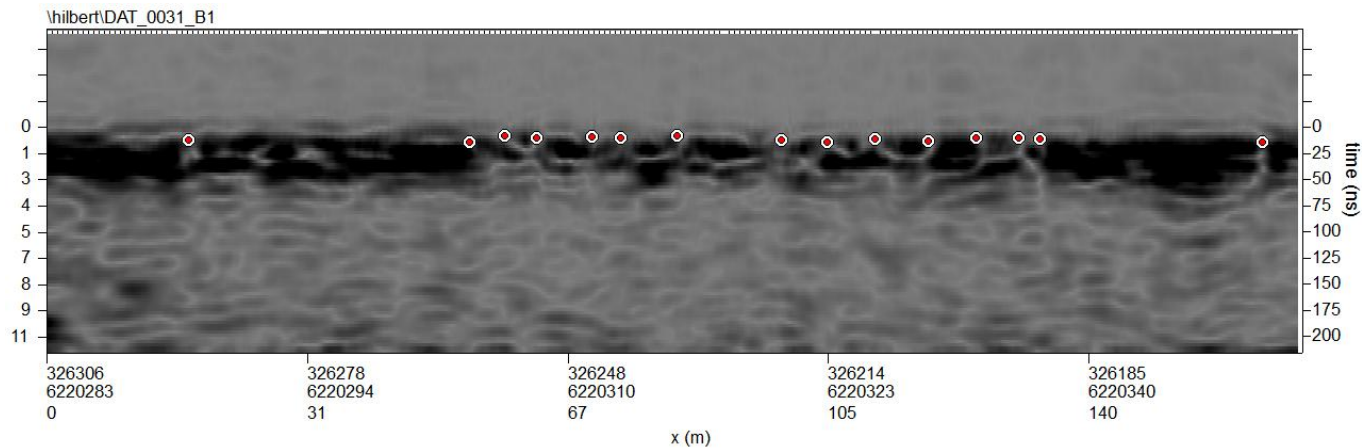


Advanced processing

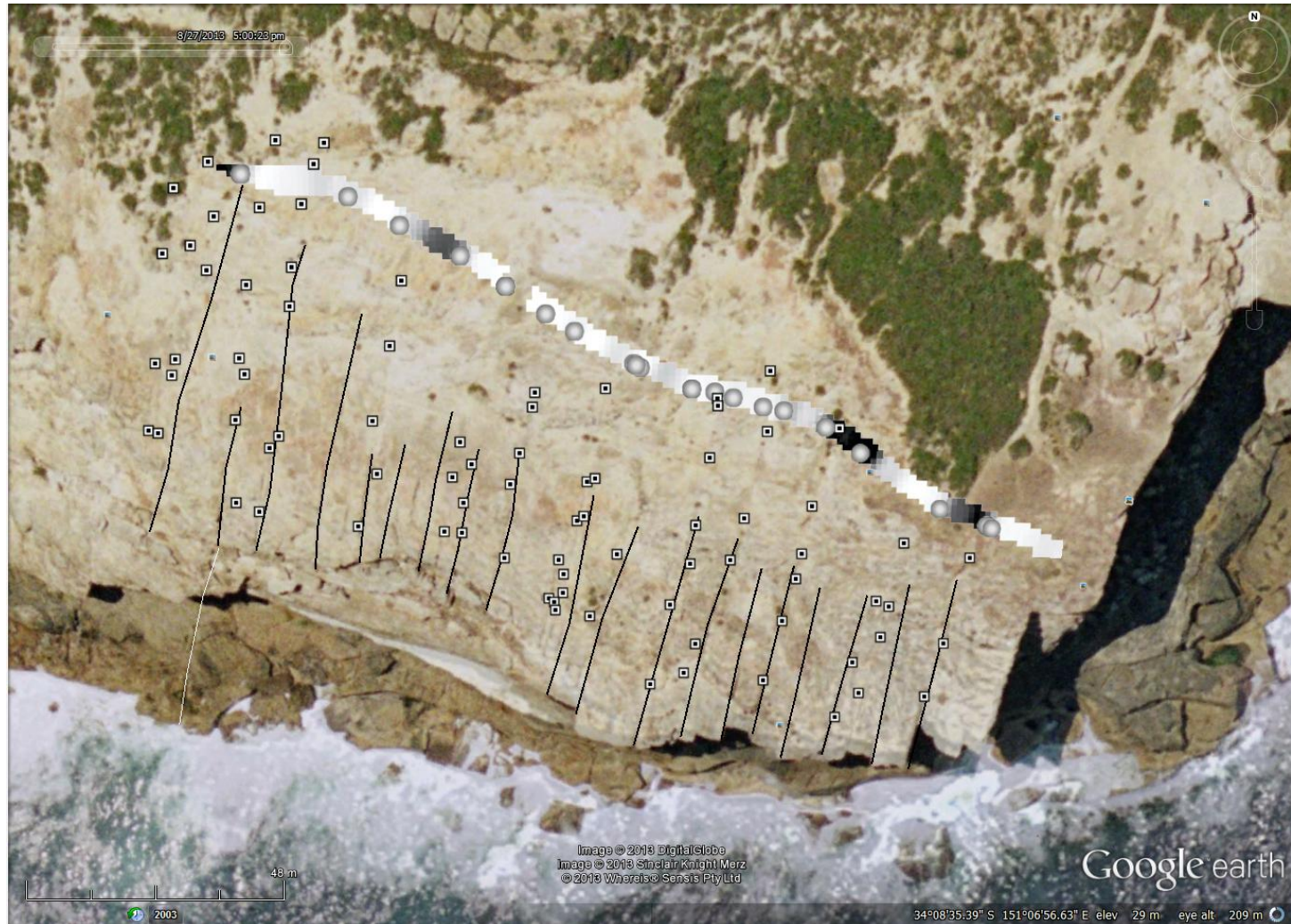


Surface fracture alignment

- Any air filled fractures should give no reflection in top section of the GPR profile
- Null amplitude spots in a Hilbert Transformed profile should correlate to air filled fractures (Patterson & Cook, 2001), (Porsani ,2006)



Royal National Park South Survey site with Mapped fractures and picked fractures from GPR profile



Identifying fractures in radargrams

- Modelling by Leucci et al (2007)
- Termination points may cause clear diffractors
- Vertical interfaces can be seen as hyperbolae diffractors
- Fractures are not perfectly straight like modelled
- Will be jagged in situ, so will appear as multiple diffractors in profile

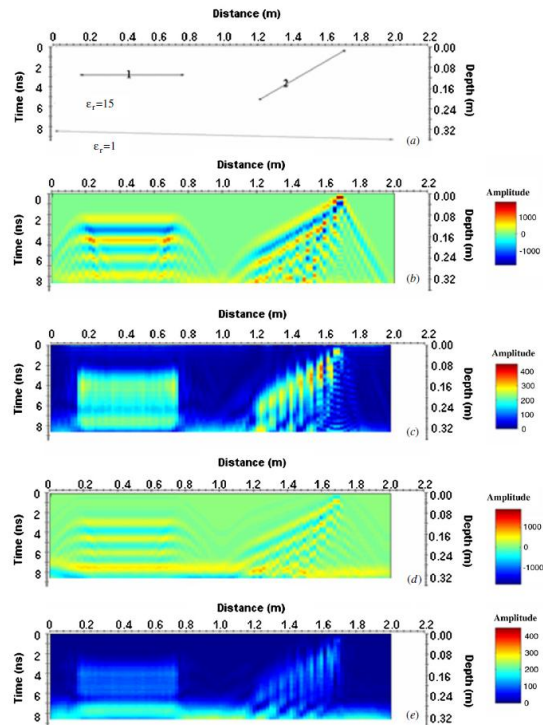
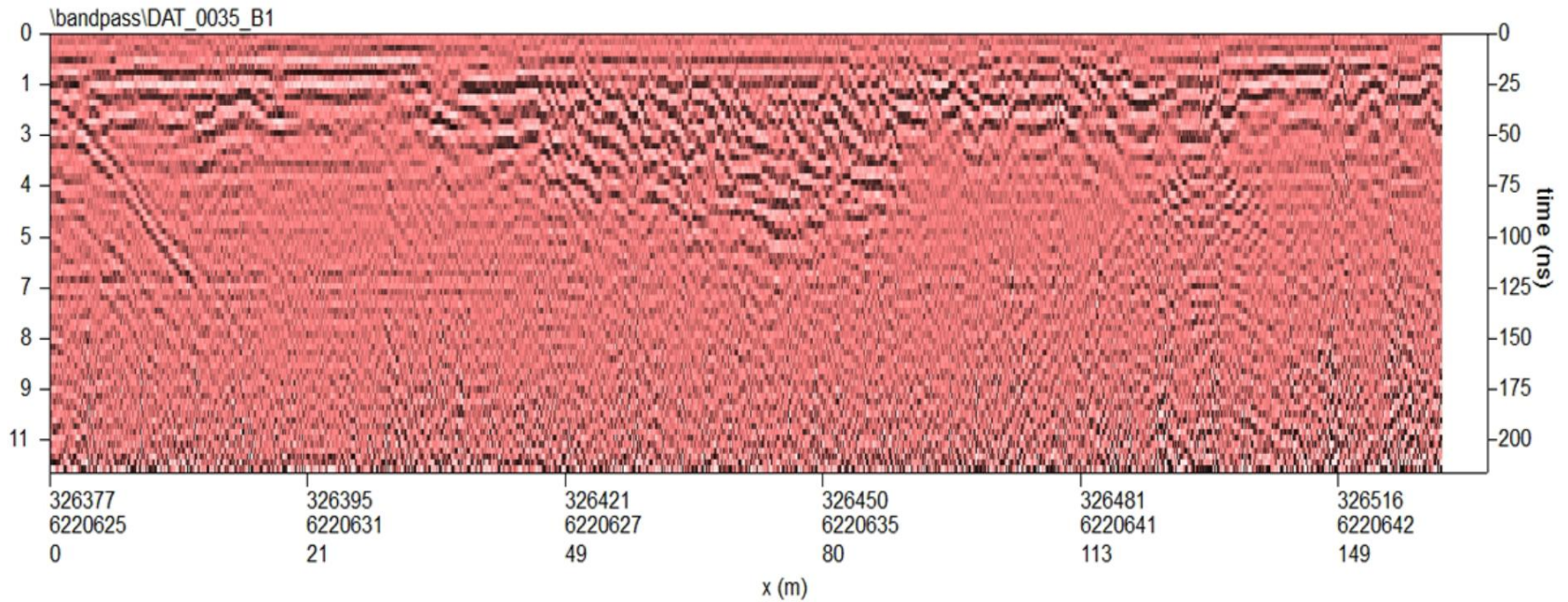
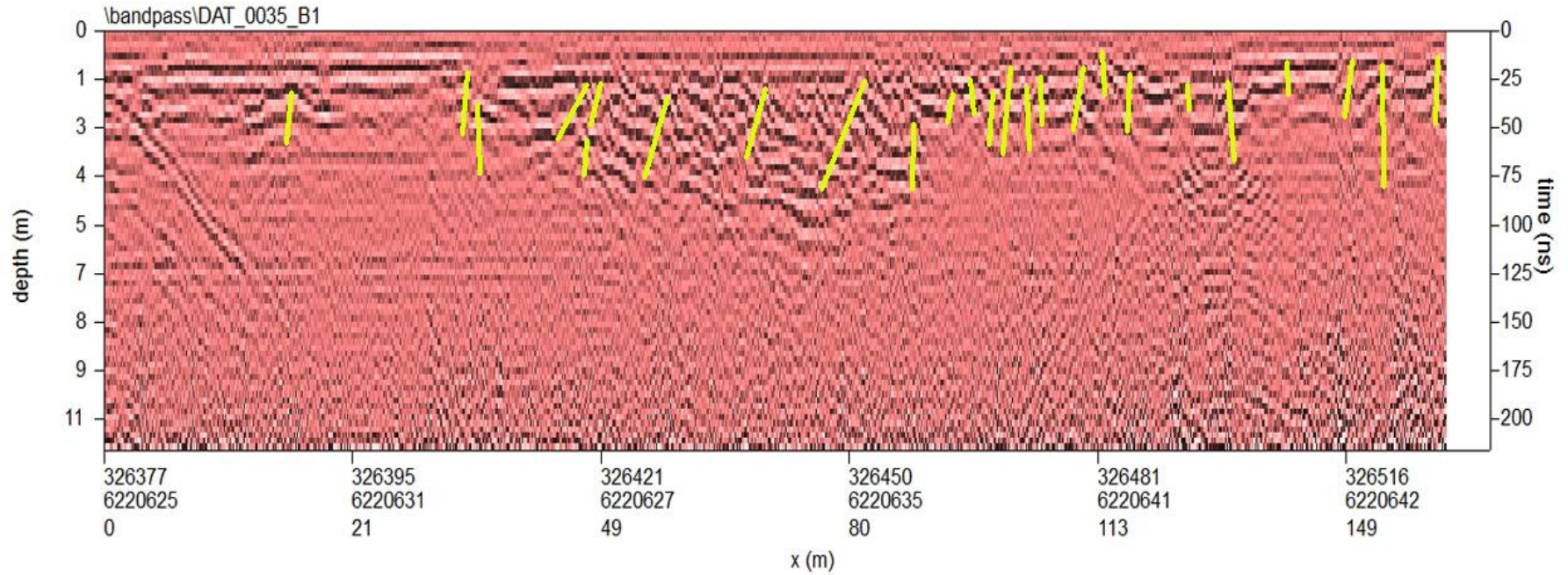


Figure 3. Synthetic data: (a) model, (b) raw data with air-filled fracture, (c) time domain processed data with air-filled fracture, (d) raw data with moist-material-filled fracture and (e) time domain processed data with moist-material-filled fracture.

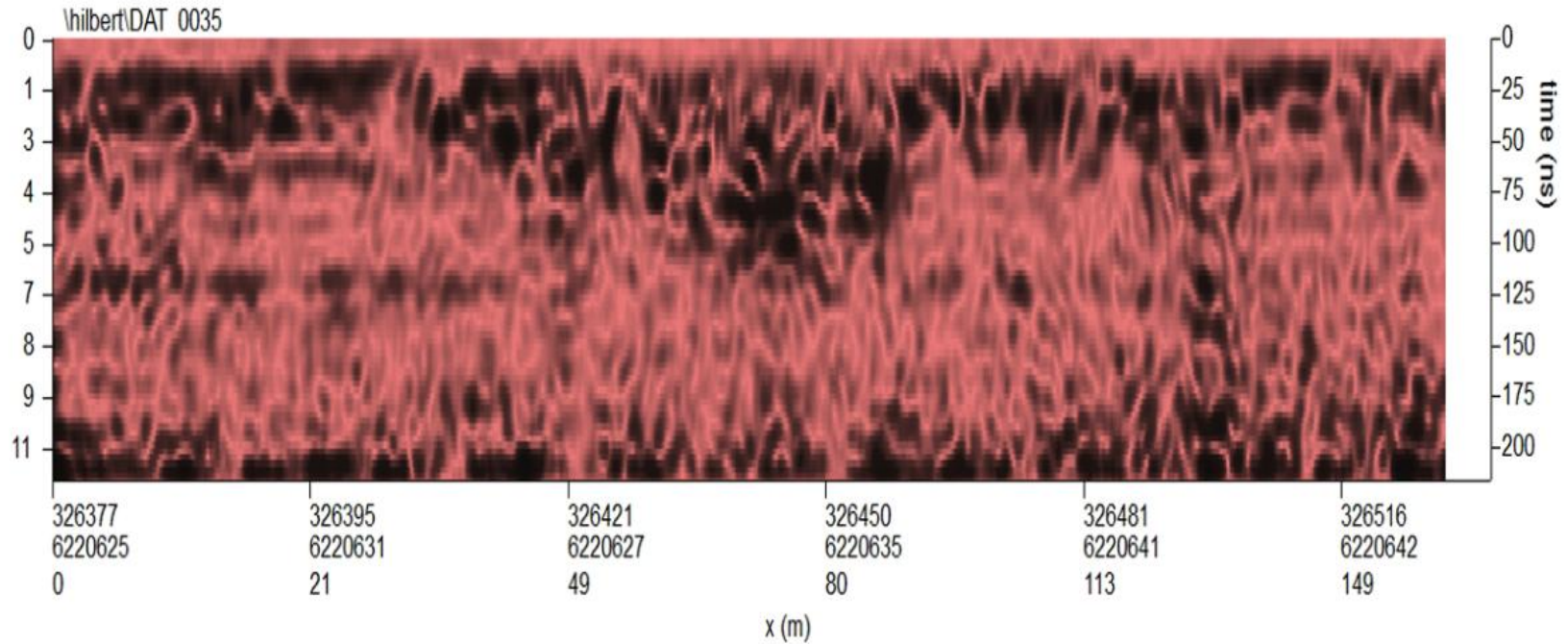
Basic Processing 100 MHz



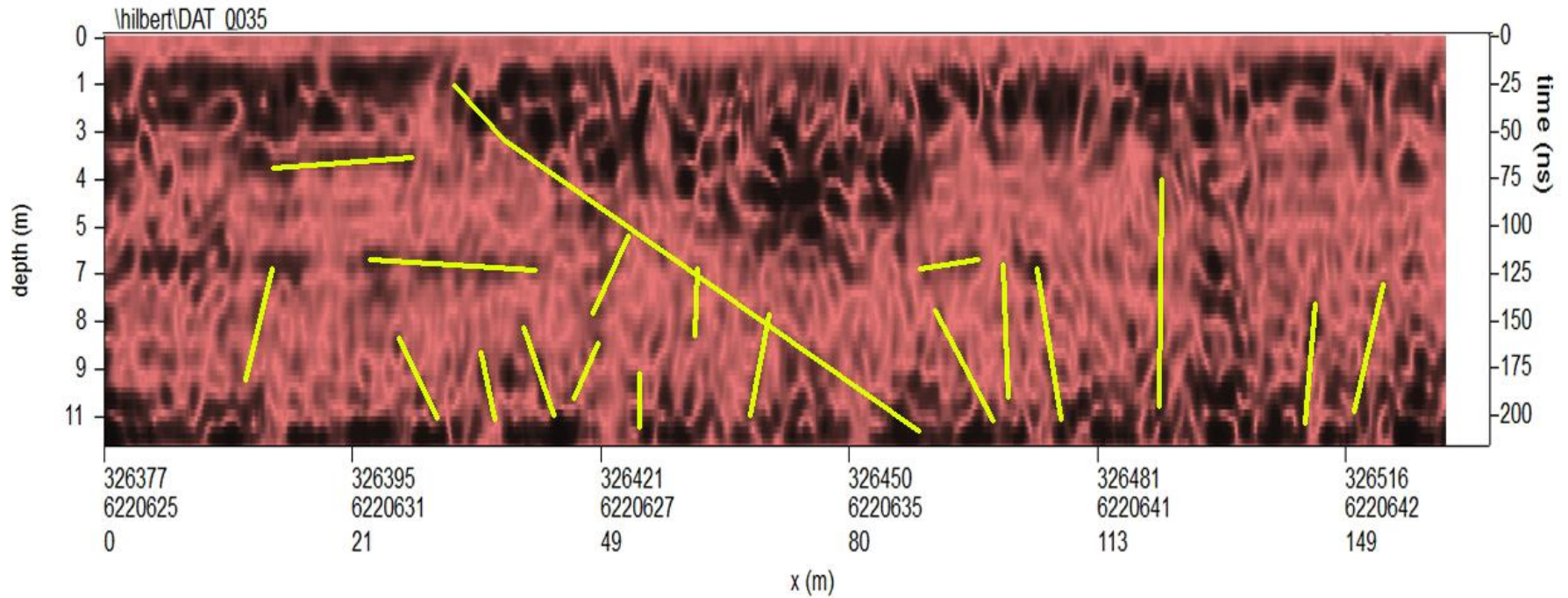
Picked discontinuous events



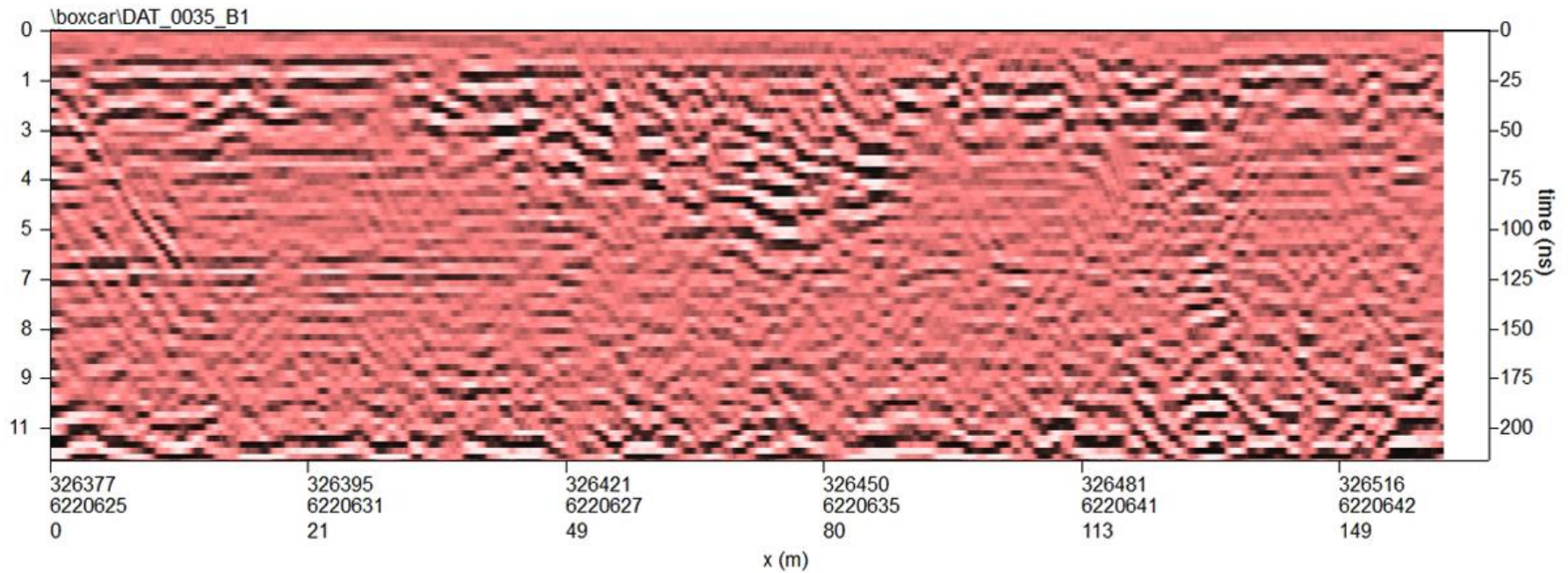
Hilbert Transformed 100 MHz



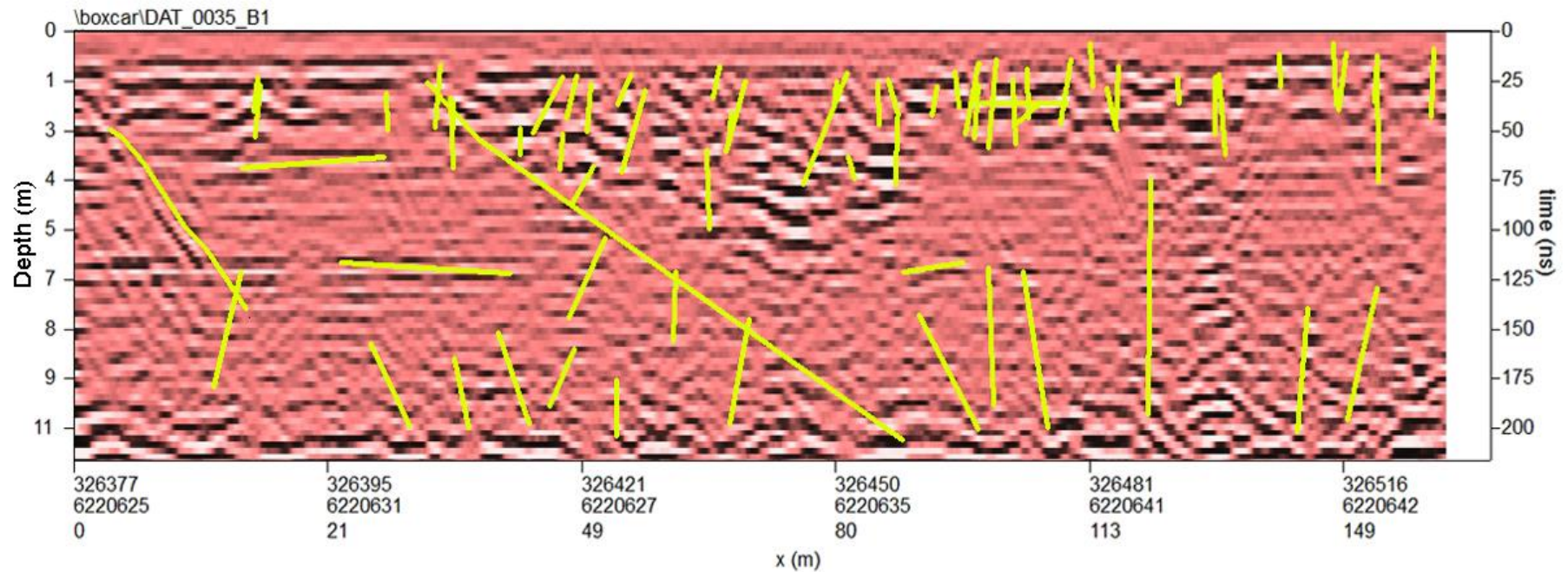
Picked discontinuous events



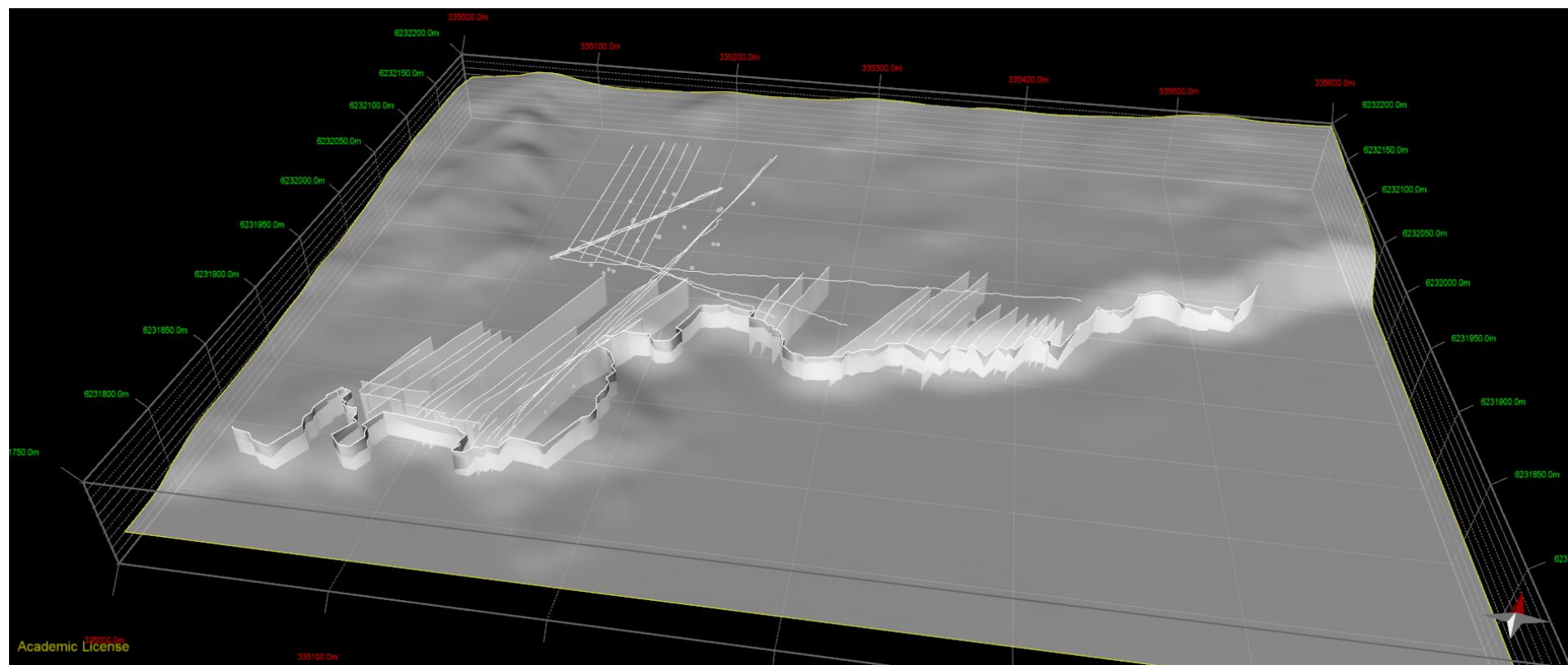
Stacked Profile 100 MHz



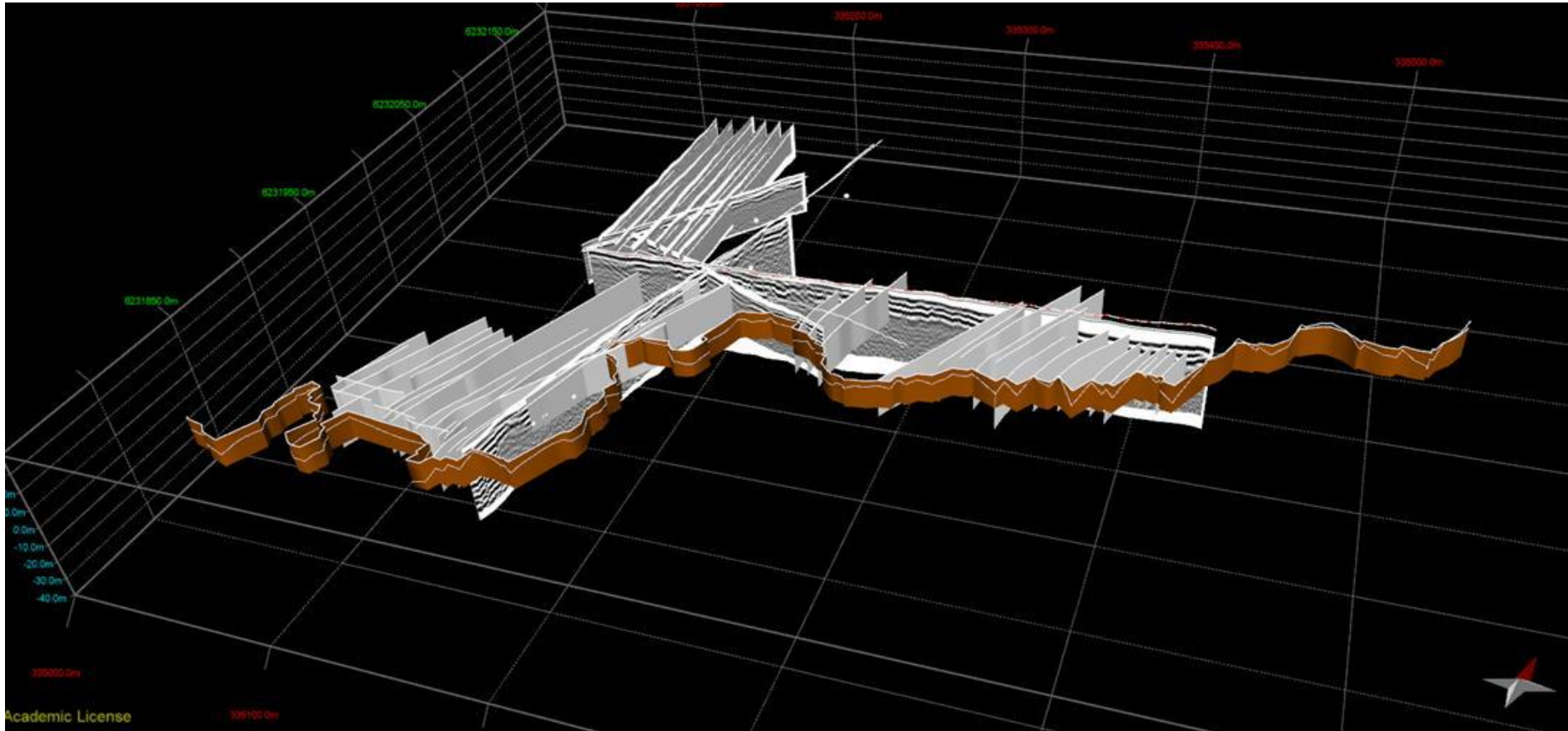
Advanced processed with all picked events



Fractures in MOVE



Fractures in MOVE



Conclusion

- On the Hawkesbury Sandstone it is estimated that the 100 MHz system penetrated to approximately 13 metres
- The 25 MHz system penetrated to approximately 25 metres .
- Major surface fractures aligned with anomalies observable in the GPR profiles.
- Using GPR it was possible to identify major subsurface fractures, and major bedding planes.
- It is unlikely that GPR systems could be used to map the complete 3D fracture network.
- It is not a simple process to map the fracture in the upper 10 m using GPR.
- Further work is required on the optimal processing steps.

References

- Heikkinen, E. & Kantia, P., 2011. *Suitability of Ground Penetrating Radar for Locating Large Fractures*, Eurajoki, Finland: Posiva Oy.
- Leucci, G., Persico, R. & Soldovieri, F., 2007. Detection of fractures from GPR data : the case history of the Cathedral of Otranto. *Journal of Geophysics and Engineering*, Volume 4, pp. 452-461.
- Memarian, H. & Fergusson, C. L., 2003. Multiple fracture sets in the southeastern Permian-Triassic Sydney Basin, New South Wales. *Australian Journal of Earth Sciences*, Volume 50, pp. 49-61.
- Shepherd, J. & Huntington, J. F., 1981. Geological Fracture Mapping in Coalfields and the Stress Fields of the Sydney Basin. *Journal of the Geological Society of Australia*, Volume 28, pp. 299-309.

Questions?

